

Investigation of solidification behavior and associate microstructures of Co–Cr–W and Co–Cr–Mo alloy systems using DSC technique

R. Liu · S. Q. Xi · S. Kapoor · X. J. Wu

Received: 3 April 2010 / Accepted: 14 June 2010 / Published online: 23 June 2010
© Springer Science+Business Media, LLC 2010

Abstract This article presents a study of solidification behavior and the corresponding microstructure of Co–Cr–W and Co–Cr–Mo alloy systems using the differential scanning calorimetry technique. The influence of main constituents on the solidification behavior and associate microstructures of these alloys are investigated. It is found that chemical composition influences significantly the solidification behavior of cobalt-based alloys. Solution-strengthened alloy has the highest solidification temperature and narrowest solidification range. Presence of carbon decreases the solidification temperature and increases the solidification range. Addition of boron greatly decreases the solidification temperature. Carbon content dominates the solidification behavior of cobalt-based alloys when the contents of the solution-strengthening elements Mo and Ni are within their saturation in the solution matrix. However, as these contents reach a certain level, formation of intermetallic compounds changes the solidification behavior of these alloys remarkably. Increase in the contents of solution-strengthening elements reduces the solid solution transformation temperature and the eutectic temperature when carbon content is constant.

Introduction

Superalloys are imperative materials for high stress, high temperature, and severe wear and corrosion environments, which are used widely in various industries [1, 2]. Solidification behavior of these alloys is closely related to their chemical compositions and dominates their microstructures that determine their various properties such as mechanical and tribological properties. Therefore, solidification processes and main influence factors of superalloys have been extensively studied; some of the research is newly reported [3–6]. Cobalt-based superalloys make up an important group of superalloy family. They are commonly used as wear-resistant materials for industrial applications involving unlubricated systems or elevated temperatures. A substantial enhancement in mechanical properties of these alloys is attributed to the crystallographic nature of cobalt (Co) [1]. The main constituent elements of cobalt-based alloys are chromium (Cr), molybdenum (Mo), tungsten (W), nickel (Ni), silicon (Si), and carbon (C). Chromium has a dual function in cobalt-based alloys; it is of vital importance in precipitation strengthening as it is the predominant carbide former, that is, most of the carbides are chromium-rich, and it is also the most important alloying element in the matrix, where it provides added strength as a solute and resistance to corrosion and oxidation [2]. Tungsten and molybdenum serve to provide additional strength to the matrix, owing to the virtue of their large atomic size. When present in large quantities, they participate in the formation of carbides during alloy solidification and promote the precipitation of M_6C ; molybdenum may also form intermetallic compounds with cobalt [7]. In addition, tungsten and molybdenum improve general corrosion resistance of the alloys [2]. Nickel has the similar function to molybdenum and tungsten as a

R. Liu (✉) · S. Q. Xi · S. Kapoor
Department of Mechanical and Aerospace Engineering, Carleton University, 1125 Colonel By Drive, Ottawa, ON K1S 5B6, Canada
e-mail: rliu@mae.carleton.ca

X. J. Wu
Institute for Aerospace Research, National Research Council of Canada, 1200 Montreal Road, Ottawa, ON K1A 0R6, Canada

solution-strengthening element; but it can also stabilize the fcc phase, thus suppressing the transformation to hcp phase of cobalt at low temperatures [8]. Carbon content varies up to 3 wt% in cobalt-based alloys. The chief difference among individual carbon-containing wear-resistant alloys is carbon content and, thus, carbide volume fraction in the alloys [9–11]. Silicon forms Laves phase with molybdenum in Tribaloy alloys, when added at levels in excess of their solubility limit with the objective of inducing the precipitation of the hard and corrosion-resistant Laves phase [12–14]. Carbon is held as low as possible in these alloys to discourage carbide formation. However, for carbide-strengthened alloys, keeping a certain level of silicon is mostly the need of processing. For example, when cobalt-based alloys are deposited as coatings by the plasma transferred arc (PTA) welding process, the presence of silicon can intake oxygen to form silicon oxide covering the PTA layer, thus protecting the layer from oxidation. In some cases, silicon also comes from ore materials. Other elements may also be added to cobalt-based alloys for special purposes, for example, addition of boron (B) can decrease the melting point of the alloy, thus reduce the required temperature for the furnace. On the other hand, owing to the feature of low-melting point, the presence of boron can enhance the mobility of the alloy during the hardfacing welding process [15, 16].

The solidification behavior of cobalt-based alloys is very complex due to the multi-element constitution, but it is very important for design and manufacturing of these alloys. The constituent elements and their contents affect the solidification behavior of these alloys, thus their microstructures, and final material properties. Solidification temperature and solidification range are the basis of casting and welding process design of an alloy. For example, the pouring temperature in a casting process is determined based on the solidification temperature and solidification range of the alloy such that the temperature should insure the alloy in liquid state during the entire molding process. If the temperature is lower, solidification would occur during the pouring, which results in the failure of the casting process. However, if the alloy liquid is overheated, the mold will be heated by the high-temperature liquid during the molding, which increases the cooling time of the cast product, leading to high thermal stresses. In general, it is desired to have a narrow solidification range for an alloy to be cast and welded. If the range is larger, the primary phase would grow freely in the liquidus alloy until the solidification process is complete. This would cause some areas of the mold unfilled for a cast product and also result in an inhomogeneous microstructure. In this research, the solidification behavior of nine Co–Cr–W alloy systems and five Co–Cr–Mo alloy systems were studied utilizing the differential scanning calorimetry (DSC) technique. The

effects of the constituent elements and their contents on the phase transformation temperature, solidification temperature, and solidification range were investigated. The associate microstructures of the alloys were analyzed. These results are useful for material engineers in design of new cobalt-based alloys and their manufacturing processes.

Experimental procedure

Samples for DSC test

Nine Co–Cr–W alloy systems and five Co–Cr–Mo alloy systems, which were developed at Deloro Stellite Group recently, were studied in this research. These alloys can be used for various purposes, such as cast products, powder metallurgy parts, PTA hardfacing layers, and high-velocity oxygen fuel (HVOF) coatings. Their chemical compositions (wt%) are listed in Tables 1 and 2, respectively. These alloys have a chromium content between 18 and 30%. In the Co–Cr–W alloy systems the tungsten content is between 4 and 15%, alloy 5A–alloy 9A also contain nickel with a content between 10 and 22%, all the alloys contain carbon and silicon except alloy 9A, and alloy 5A–alloy 7A contain an additional element, boron. In the Co–Cr–Mo alloy systems the molybdenum content is between 6 and 28%, the nickel content is between 4 and 28%; these alloys

Table 1 Chemical compositions (wt%) of Co–Cr–W alloy systems

Element:	Cr	W	Ni	Si	C	B	Co
Alloy							
1A	30	9		1.5	1.6		Bal.
2A	30	9		1.5	2		Bal.
3A	28	4		1.3	1.3		Bal.
4A	28	4		1.3	1.7		Bal.
5A	19	13	13	2.8	1.5	2.5	Bal.
6A	19	8	13	2.6	0.8	1.8	Bal.
7A	19	8	13	2.9	1.1	1.8	Bal.
8A	25	13	22	1.2	1.8		Bal.
9A	20	15	10				Bal.

Table 2 Chemical compositions (wt%) of Co–Cr–Mo alloy systems

Element:	Cr	Mo	Ni	Si	C	B	Co
Alloy							
1B	24	12	4	0.2	0.55		Bal.
2B	27	6	4	0.4	0.25		Bal.
3B	18	28	10	3.2			Bal.
4B	18	23	16	2.8			Bal.
5B	18	6	28	1.8		3.5	Bal.

all contain silicon, but alloy 1B and alloy 2B contain a low level of silicon and also contain a low level of carbon; the others contain a high level of silicon; alloy 5B contains boron as well. Each sample of the alloys was provided in powder state by Deloro Stellite Group, and a small amount of each powder sample weighing around 80 mg was used for the DSC test.

DSC test

Differential scanning calorimetry test was conducted on each alloy sample with a DSC 404C instrument, which can detect and qualify almost all calorimetric effects that occur in materials. The heating/cooling cycle used in this research is illustrated in Fig. 1. The maximum heating temperature is 1,500 °C owing to the high-melting point of Co. The samples were heated to 100 °C and kept for 20 min. Then they were heated again up to the ultimate temperature, kept for 10 min, and cooled down to room temperature with the same rate of 10 °C/min. The phase transformation behavior of the material during the heating and cooling processes is characterized by the DSC curve that is recorded automatically in the test.

Microstructural analysis

The solidified samples after the DSC test were microstructurally analyzed under an optical microscope. The samples were first hot mounted in a plastic base, followed by a series of polishing step as follows. The surface was ground with grit papers from course #180 to fine #600 and polished with abrasive cloth plus 1 μm alumina powders. The polished surfaces were then etched electrolytically using an aluminum cathode at a voltage of 3 V for about

10 s. The etchant is a mixed solution containing 9 g CrO₃, 15 mL HCl, and 150 ml H₂O.

Experimental results

DSC curves

The DSC curves obtained from the solidification (cooling) process for the two groups of alloys are presented in Figs. 2 and 3. The critical data corresponding to phase transformation temperatures are summarized in Tables 3 and 4. T_s is defined as solidification temperature, that is, the temperature at which the largest exothermic peak occurs. T_b and T_a are the temperatures at which the exothermic peaks before and after the largest peak occur, respectively. ΔT is defined as solidification range, which is the temperature range between the start of solidification (the first exothermic peak) and the end of the largest exothermic peak.

For the Co–Cr–W alloy systems, firstly, consider alloy 9A, which contains no C so that it is a solution-strengthened alloy. As demonstrated by its DSC curve in Fig. 2d, it has the highest solidification temperature and the narrowest solidification range among the alloys being discussed. It only has single exothermic peak representing the cobalt solid solution formation. Secondly, compare alloy 1A–alloy 4A with alloy 9A. Due to the presence of C, the solidification temperatures of these alloys are apparently lower than that of alloy 9A, see Fig. 2a, b. Moreover, additional exothermic peaks appear on their DSC curves; the peak before the largest exothermic peak represents the primary solid solution formation; the peak after represents the precipitation of the carbide; the largest exothermic peak is for the eutectic transformation. Alloy 1A and alloy 2A have similar chemical compositions so that the solidification temperatures of the two alloys are almost same, but the solidification range of alloy 1A with less C is wider. Alloy 3A and alloy 4A have similar compositions but alloy 4A contains higher C. Between these two alloys, the former has a slightly higher solidification temperature but narrower solidification range, as seen in Fig. 2b. Alloy 1A–alloy 4A have same constituents, Co, Cr, W, Si, and C, but the contents of these elements vary among the alloys. Alloy 3A and alloy 4A contain lower levels of Cr, W, Si and C than alloy 1A and alloy 2A; see Table 1. With these differences, alloy 3A and alloy 4A have higher solidification temperatures, higher primary phase transformation temperatures and wider solidification ranges. No secondary carbide precipitation occurs in these alloys, because no peaks after the largest exothermic peak are observed on their DSC curves. Thirdly, compare alloy 8A with alloy 1A–alloy 4A. This alloy contains an additional element, Ni, and lower Cr but higher W, see Table 1. Accordingly,

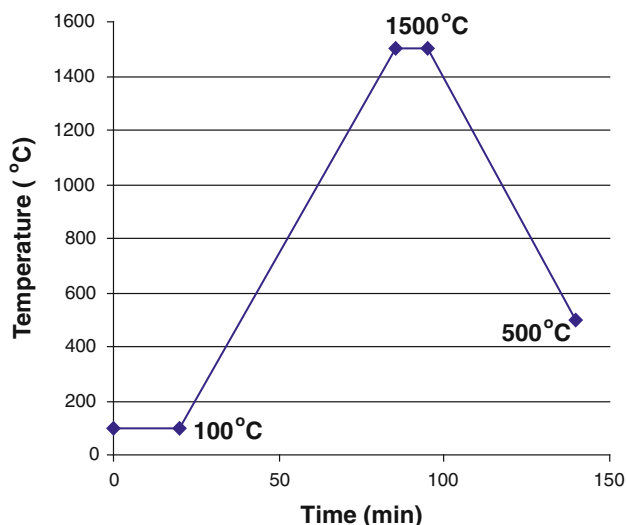


Fig. 1 DSC heating/cooling cycle

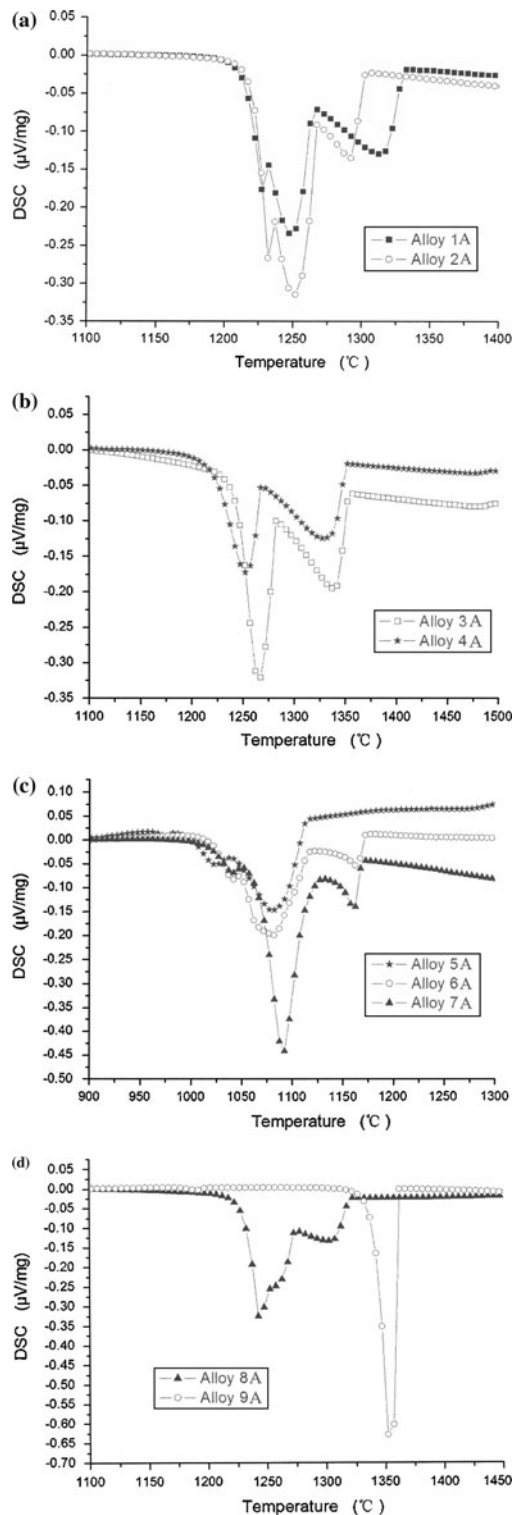


Fig. 2 DSC curves of **a** alloy 1A and alloy 2A, **b** alloy 3A and alloy 4A, **c** alloy 5A–alloy 7A, and **d** alloy 8A and alloy 9A

it has similar solidification behavior to alloy 3A and alloy 4A, see its DSC curve in Fig. 2d, but it has a slightly lower solidification temperature than these alloys, as seen in

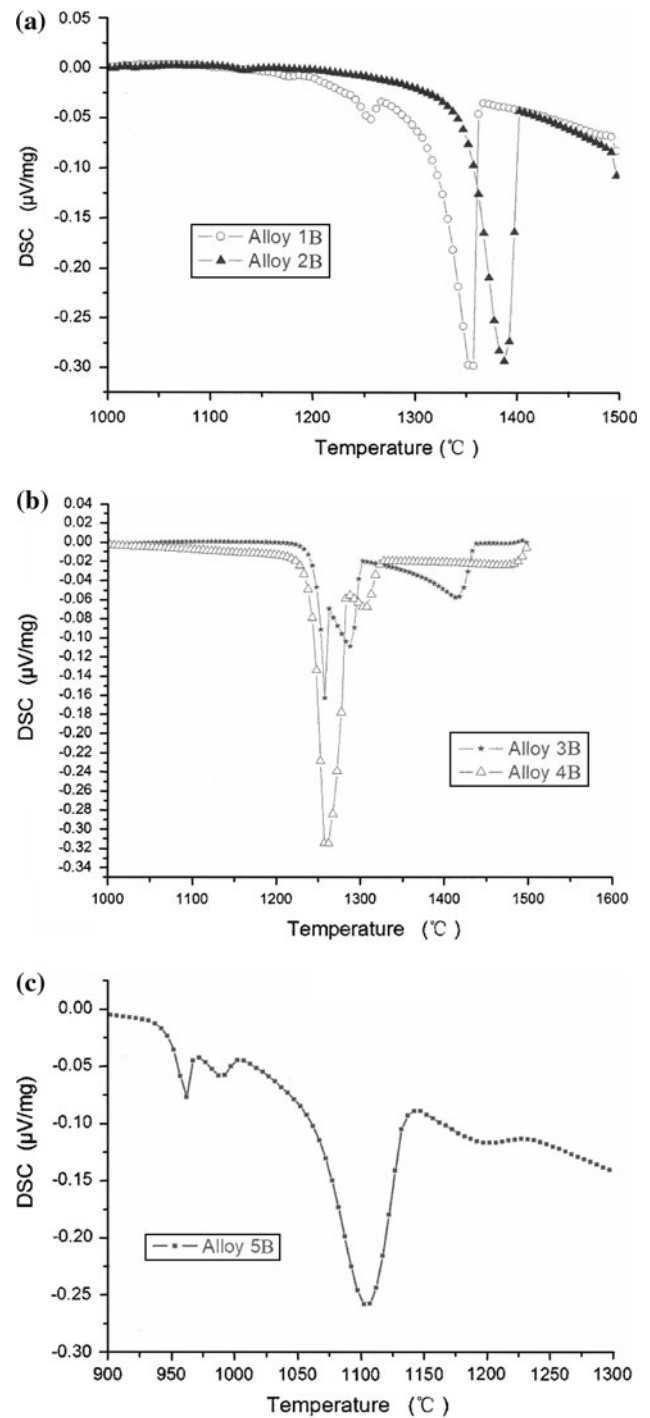


Fig. 3 DSC curves of **a** alloy 1B and alloy 2B, **b** alloy 3B and alloy 4B, and **c** alloy 5B

Table 3. Its solidification range is wider than those of alloy 1A and alloy 2A but narrower than those of alloy 3A and alloy 4A. Finally, alloy 5A–alloy 7A have similar compositions, in addition to Co, Cr, W, Ni, Si, and C, these alloys also contain B. The significant difference in solidification behavior of these alloys from the alloys discussed

Table 3 DSC test data of Co–Cr–W alloy systems

Alloy	T_s (°C)	T_b (°C)	T_a (°C)	ΔT (°C)
1A	1250	1312	1225	98
2A	1251	1292	1232	68
3A	1268	1337		130
4A	1255	1326		151
5A	1078		1020, 980	75
6A	1078	1165	1040	125
7A	1095	1160	1040	124
8A	1240	1320		114
9A	1352			38

Table 4 DSC test data of Co–Cr–Mo alloy systems

Alloy	T_s (°C)	T_b (°C)	T_a (°C)	ΔT (°C)
1B	1355		1255	58
2B	1388			53
3B	1260	1415, 1290		205
4B	1260	1305		105
5B	1100		988, 960	110

previously is that their solidification temperatures are very low, as seen in Fig. 2c. These B-containing alloys also contain a higher level of Si, as shown in Table 1. Alloy 6A and alloy 7A have similar solidification behavior, but the solidification temperature of alloy 7A, which contains higher Si and C, is slightly higher. These alloys have exothermic peaks before and after the largest exothermic peak, which means that there is a primary phase solidified in the liquidus state and also secondary precipitation occurs in the solidus state in these alloys. For alloy 5A, since the largest exothermic peak occurs first, this alloy may be a eutectic alloy; the eutectic product can be a mixture of the Co solid solution, carbides, silicides, and borides. Due to the two exothermic peaks after the largest exothermic peak, secondary precipitation would occur in this alloy.

Regarding the Co–Cr–Mo alloy systems, firstly, consider alloy 2B. This alloy contains low C (0.25 wt%); therefore, it is nearly a solution-strengthened alloy. Accordingly, its DSC curve has single exothermic peak, which represents the cobalt solid solution transformation; see Fig. 3a. There should be carbides precipitated in the solution matrix with the eutectic reaction [7], however, as the carbide amount is very small, the exothermic peak is too weak to be visualized on the DSC curve. Secondly, compared with alloy 2B, alloy 1B contains double C and Mo; see Table 2, so that on its DSC curve after the largest exothermic peak (Co solid solution transformation) there is a small exothermic peak, which stands for the eutectic reaction; see Fig. 3a. The eutectic products consist of carbides and intermetallic compounds [7] that are

attributed to the higher Mo content. It should be noticed that in this alloy solid solution still takes most percentage of the volume. As demonstrated by its DSC curve that the solid solution transformation peak is much larger than the eutectic formation peak; this is due to the lower C content. However, for carbide-strengthened cobalt-based alloys, when the C content is great than 1 wt%, the eutectic reaction predominates the solidification process [17, 18]. As a result, the largest exothermic peak occurs for the eutectic reaction, not for the solid solution transformation. Comparing the DSC curves between alloy 1B and alloy 2B, the latter with less amount of C has a higher solidification temperature and narrower solidification range, see Table 4. Thirdly, alloy 3B and alloy 4B have same constituents; they do not contain C but contain a high level of Si. Due to the coexistence of Mo and Si, intermetallic compound, CoMoSi or Co₃Mo₂Si Laves phase, is formed in these alloys, that is, they are Triballoy alloys. Since both the Mo content and the Si content are high, these alloys are hypereutectic with the primary phase being the Laves phase. As demonstrated on their DSC curves in Fig. 3b, there are two peaks for alloy 3B and one peak for alloy 4B before the largest exothermic peak, which represent the primary Laves phase transformations; the largest exothermic peak represents the eutectic reaction, which results in a eutectic product of the Co solid solution and the Laves phase. These two alloys have a same solidification temperature, but alloy 3B, containing higher Mo and Si, has two primary Laves phase transformations with one occurring at a higher temperature, which makes the solidification range of this alloy wider, as seen in Table 4. Finally, compared with alloy 3B and alloy 4B, alloy 5B contains additional element, B, and it contains lower Mo and Si but higher Ni. With these differences, its solidification behavior deviates significantly from that of alloy 3B and alloy 4B, as seen in Fig. 3c. The solidification temperature of alloy 5B decreases significantly due to the presence of B. The largest exothermic peak occurs first, followed by two small peaks in this alloy. Owing to the low Mo content, the CoMoSi or Co₃Mo₂Si Laves phase may not form in this alloy, but the presence of Si may result in intermetallic compounds with the high amount of Ni. This alloy is possibly a eutectic alloy according to its chemical composition and DSC curve; the largest exothermic peak represents the eutectic reaction and the small peaks represent secondary precipitation of silicides and borides. The solidification range of alloy 5B is close to that of alloy 4B, see Table 4.

Microstructures

For the Co–Cr–W alloy systems, as mentioned above, alloy 9A contains no C so that it is a solution-strengthened alloy.

In correspondence to its DSC curve, the microstructure obtained under an optical microscope in Fig. 4a has confirmed that this alloy consists of single phase of cobalt solid solution. Compared with alloy 9A, alloy 1A–alloy 4A contain a high level of C and these alloys are hypoeutectic and have similar microstructures, with the primary phase being cobalt solid solution having a dendritic structure and the eutectic being a mixture of solid solution and Cr-rich carbides, as shown in Fig. 4b. This is a typical microstructure of Stellite alloys with Co–Cr–W [1]. The eutectic also includes silicon compounds due to the moderate Si content. This has been confirmed by the composition analysis using backscatter electron imaging and energy dispersive X-ray (EDX) spectrum in a Hitachi Model S-570 scanning electron microscope (SEM). This microstructure agrees with their DSC curves as that the peak occurring before the largest exothermic peak represents the transformation of the cobalt solid solution and the largest exothermic peak stands for the eutectic formation. For alloy 8A, it has a similar composition to alloy 3A and alloy 4A but it contains a high content of additional element, Ni, lower Cr but higher W. Accordingly, its microstructure shown in Fig. 4c consists of primary solid solution in a dendritic structure and the eutectic in fishbone shape. Alloy 5A–alloy 7A contain the same constituents, especially they all contain B. Besides B, these alloys also contain a higher content of Si, compared with the other alloys. Alloy 6A and alloy 7A have similar compositions except that the latter contains higher C and Si. Comparing their DSC results, these two alloys have very similar solidification behavior, so do the microstructures. The peak before the largest exothermic peak indicates that there is a primary phase formed before the eutectic solidification in these alloys. According to the microstructure shown in Fig. 4d, these alloys are hypereutectic with the primary phase being silicon compounds in needle shape, which has been confirmed by the result of EDX/SEM. The eutectic product is a mixture of the solid solution, carbides, borides, and silicon compounds as well. The primary silicon-compound phase is attributed to the high level of Si present. The peak after the largest exothermic peak indicates secondary precipitation occurring in these alloys; the precipitates may mainly be boride because B has a lower eutectic temperature, but secondary precipitation of carbide is also possible. However, alloy 5A exhibits different solidification behavior from alloy 6A and alloy 7A. As seen in Fig. 2c, the largest exothermic peak occurs first on its DSC curve. Incorporating with its microstructure shown in Fig. 4e, this alloy is a eutectic alloy. The eutectic product has a laminate structure, consisting of the solid solution and carbon, silicon, and boron compounds; these compositions have been proven by the EDX/SEM result. There is also secondary precipitation occurring in this alloy, as seen in the

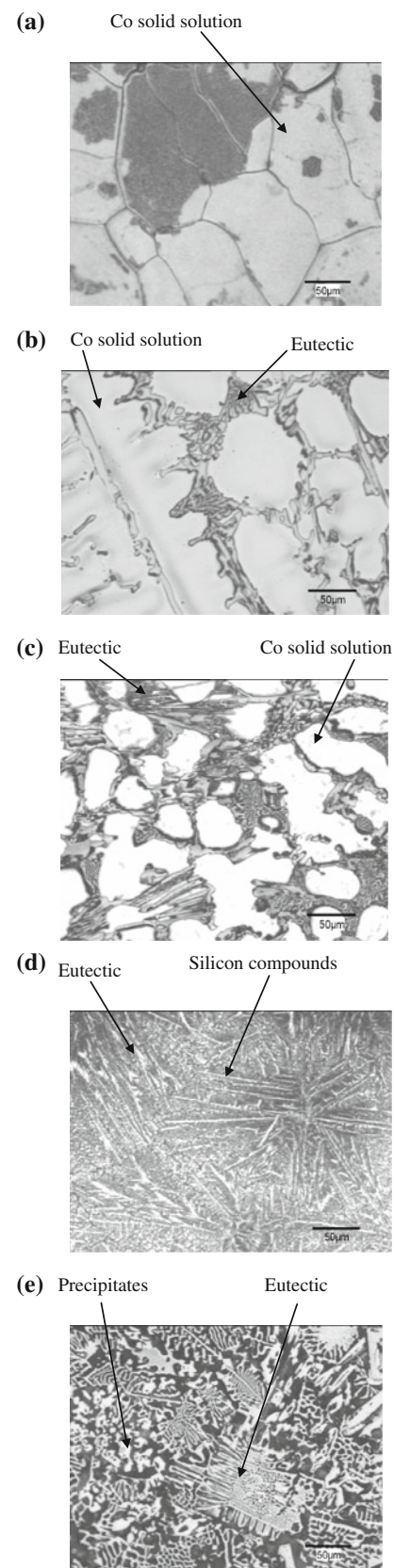


Fig. 4 Microstructures of **a** alloy 9A, **b** alloy 3A, **c** alloy 8A, **d** alloy 6A, and **e** alloy 5A

microstructure, which corresponds to the small peaks after the largest exothermic peak on its DSC curve. The precipitates are mainly Cr-rich borides due to the lower eutectic temperature of B, which is demonstrated by the EDX/SEM result.

For the Co–Cr–Mo alloy systems, since alloy 2B contains a low content of carbon, its microstructure consists of major dendritic Co solid solution and minor carbides in the eutectic mixture; see Fig. 5a. This is a typical microstructure of Stellite alloys with low carbon; the carbides are Cr_7C_3 and Cr_{23}C_6 ; the Cr_7C_3 carbides are eutectic with the Co solid solution, while the Cr_{23}C_6 carbides are a precipitate in fishbone shape [1, 7]. With the increase in C and Mo contents, alloy 1B contains more carbides than alloy 2B; it also contains intermetallic compounds (Co_3Mo and Co_7Mo_6) due to the higher Mo content [7], as seen in Fig. 5b (the carbides are in black and the intermetallic compounds are in gray). Due to the presence of high contents of Mo and Si, alloy 3B and alloy 4B contain a large volume fraction of Laves phase. These two alloys have the similar microstructure consisting of the primary Laves phase in a dendritic structure and the Co solid solution in the eutectic mixture, as shown in Fig. 5c. This microstructure is a typical microstructure of Triballoy alloys [1]. The difference in chemical composition between these two alloys is that alloy 3B contains more Mo and Si, which results in a larger volume fraction of Laves phase. Accordingly, the DSC curve of alloy 3B has two peaks before the largest exothermic peak, representing two transformations of the large amount of Laves phase, while that of alloy 4B only has one. The presence of boron makes alloy 5B behave differently from alloy 3B and alloy 4B in the solidification process. It is noticed on its DSC curve that the largest exothermic peak occurs first, in correspondence with its microstructure in Fig. 5d, this alloy looks like a eutectic alloy. The eutectic product is a mixture of Si and B intermetallic compounds [19] and Co solid solution. The two small peaks on the DSC curve represent secondary precipitation of Si and B intermetallic compounds. Their compositions have been identified by the EDX/SEM. Compared with alloy 3B and alloy 4B, Mo and Si contents in alloy 5B are greatly reduced. The low Mo content depresses the formation of the CoMoSi or $\text{Co}_3\text{Mo}_2\text{Si}$ Laves phase, but the high content of Ni induces the formation of Ni–Si intermetallic compounds [20], which is confirmed by the EDX/SEM result.

Discussion

The DSC tests and microstructural analyses show that chemical composition affects significantly the solidification behavior and associate microstructure of cobalt-based

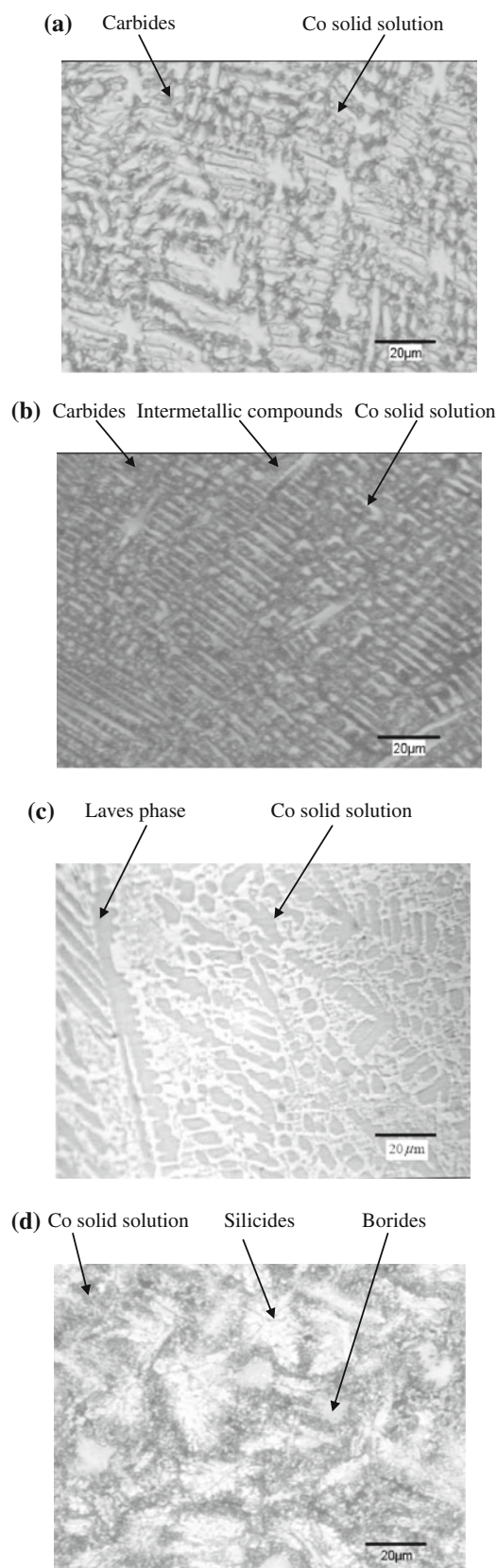


Fig. 5 Microstructures of **a** alloy 1B, **b** alloy 2B, **c** alloy 4B, and **d** alloy 5B

alloys. However, since these alloys are multi-element alloy systems, theoretical understanding of these issues has substantial difficulty due to the metallurgical complexity, although the effects of individual elements in these alloys have theoretical inhesion. The experimental studies in and results from this research may help understand these issues instead.

Effects of carbon

Carbon in wear-resistant cobalt-based alloys plays an indispensable role. The chief difference among these alloys is carbon content and, thus, carbide volume fraction in the material. For example, at a carbon level of 2.4 wt% (Stellite 3), the carbides constitute about 30 wt% of the material. These are of the M_7C_3 (chromium-rich primary) and M_6C (tungsten-rich eutectic) types, where M represents the metal component, for example, M_7C_3 corresponds to Cr_7C_3 . At 1 wt% carbon (Stellite 6B), the carbides constitute approximately 13 wt% of the material, these being predominantly chromium-rich eutectic carbides of the M_7C_3 type [1]. From the DSC tests, it is clear that carbon influences significantly the solidification behavior of cobalt-based alloys. As reported above, alloy 9A contains no C so that it is a solution-strengthened alloy. The DSC test shows that there is only single exothermic peak on its DSC curve, which corresponds to the solid solution transformation. This alloy has the highest solidification temperature and narrowest solidification range among the alloys being studied. When these alloys are cast, they would have good fluidity and properties for filling fully into the cast mold. Due to lack of C, thus carbides, this type of alloys are relatively soft and ductile so that they are commonly used for high temperature, high stress, or strength applications.

The presence of C decreases the solidification temperature and increases the solidification range, as demonstrated by alloy 1A–alloy 4A. This is easy to understand according to Co–C, Co–Cr, Co–Mo, and Co–W binary phase diagrams [21, 22]. For example, as the Co–C binary phase diagram shows, when the carbon content is within 2 wt%, the lowest solidification temperature is about 1,350 °C, while the Co–Cr binary phase diagram shows that when the chromium content is within 30 wt%, the lowest solidification temperature is about 1,460 °C. Therefore, it can be expected that the solidification temperature of Co–Cr–W alloys and Co–Cr–Mo alloys with the single transformation of liquid to solid phase is higher than that of Co–Cr–W alloys and Co–Cr–Mo alloys with carbon. Alloy 1A–alloy 4A, containing carbon, are hypoeutectic and have similar microstructures, with the primary phase being cobalt solid solution having a dendritic structure and the eutectic being a mixture of solid solution

and Cr-rich carbides, as shown in Fig. 4b. In accordance to the DSC curves, the peak occurring before the largest exothermic peak represents the transformation of the solid solution and the largest exothermic peak represents the eutectic reaction. Due to the formation of carbides, these alloys with multi-phase transformations has wider solidification range than alloy 9A with single phase transformation. Furthermore, comparing alloy 1A and alloy 2A with alloy 3A and alloy 4A, there is secondary carbide precipitation occurring in the first two alloys, because there is a peak after the largest exothermic peak on their DSC curves. This may be due to the higher Cr and C contents, which promote the secondary precipitation of Cr-rich carbides.

Effects of molybdenum

Molybdenum also influences the solidification behavior of cobalt-based alloys. It has a dual function in these alloys; it mainly remains in the solid solution to strengthen the matrix when its content is low (approximately below 8 wt%) in these alloys; but it would form intermetallic compounds with other elements when its content is high (usually above 12 up to 28 wt%). As demonstrated by alloy 1B and alloy 2B, the latter contains lower Mo (6 wt%) so that the Mo in this alloy plays the role in strengthening the solution matrix. However, as its content is increased to 12 wt%, in alloy 1B, it is found that intermetallic compounds (Co_3Mo and Co_7Mo_6) are formed [7]. Comparing the DSC curves between these two alloys, it is observed that increase in the Mo content decreases the transformation temperature of the solid solution but increases the solidification range, which agrees with the Co–Mo binary diagram [21, 22]. The feature of precipitation of intermetallic compounds, Co_3Mo and Co_7Mo_6 , is demonstrated by the small peak after the largest exothermic peak (solid solution transformation) on the DSC curve of alloy 1B.

Due to the presence of high contents of Mo and Si, alloy 3B and alloy 4B contain a large volume fraction of Laves phase. These two alloys have the similar microstructure consisting of the primary Laves phase in a dendritic structure and the Co solid solution in the eutectic mixture, as shown in Fig. 5c. However, if the Si content is lower, for example, below 2.0 wt%, hypoeutectic reaction would take place with the primary phase being Co solid solution and the Laves phase as the eutectic embedded in the solution matrix [23, 24]. The difference in chemical composition between these two alloys is that alloy 3B contains higher Mo and Si, which results in a larger volume fraction of Laves phase. Accordingly, the DSC curve of alloy 3B has two peaks before the largest exothermic peak, which represent two transformations of the large amount of Laves phase, while that of alloy 4B only has one. The eutectic

temperatures of these two alloys are the same. In general, for multi-element alloys eutectic temperature varies with the constituents and their contents, which differs from binary C or Si systems [21], and the variation may not follow a straightforward trend due to the metallurgical complexity. However, since the total contents of the solution-strengthening elements in alloy 3B and alloy 4B are very close, the Si content may have little effect on the eutectic temperature, assuming that in this case the multi-element systems are equivalent to binary Si systems when taking the total solutes as a unit.

Effects of boron

The most special feature of B is its low-eutectic temperature. As noticed from the DSC tests that addition of B reduces remarkably the solidification temperature of cobalt-based alloys. Among the alloys being studied alloy 5A–alloy 7A and alloy 5B contain different amounts of B. As seen in Figs. 2c and 3c, the solidification temperatures of these alloys are much lower than those of the others. However, it is hard to know from this research if higher B content would lead to lower solidification temperature, in other words, if the higher B content in an alloy, the lower the solidification temperature of the alloy is. Among the three alloys containing B, alloy 5B has the highest B content, but its solidification temperature is higher than those of the others. Alloy 6A and alloy 7A have the same amount of B, but they have different solidification temperatures, while alloy 5 and alloy 6 have different amounts of B, but they have the same solidification temperatures. This is because the chemical compositions of these alloys are quite different except that they all contain B. For example, alloy 5B does not contain C but contains a high level of Ni, while alloy 5A–alloy 7A contain different amounts of C and Si. These differences result in formation of different phases among these alloys, which complicates the quantitative valuation of the B effect on the solidification temperature of these alloys. Boron with chromium forms Cr-rich borides in cobalt-based alloys.

Effects of other alloying elements

Finally, consider other alloying elements in these studied alloys. As observed in the DSC tests, the solidification behavior of cobalt-based alloys is determined predominantly by carbon, boron, and their contents; the effect solution-strengthening elements can be negligible compared with those of carbon and boron when their contents are within their saturation in the solution matrix. For example, the main difference between alloy 9A and alloy 1A–alloy 4A is that the former does not contain C but the latter does. Formation of carbides results in noticeable

deviation of the solidification behavior of alloy 1A–alloy 4A from that of alloy 9A. In this case, although there is difference in the contents of the solution-strengthening elements between these alloys, the effect of this difference on the solidification change is negligible.

However, when the contents of solution-strengthening elements are excessive in cobalt-based alloys, that is, they are over their saturation in the solution matrix, some of them may precipitate from the solution to form carbides or intermetallic compounds, which will influence the solidification behavior of the alloys significantly. For example, when Mo is less, as in alloy 2B and alloy 5B, it remains in the solution matrix as a solute, but when its content reaches a certain level, as in alloy 1B, alloy 3B and alloy 4B, it precipitates from the matrix to form intermetallic compounds, which changes the solidification behavior of these alloy greatly. Similarly for Ni, as its content is excessively high, as in alloy 5B, it precipitates from the matrix to form Ni–Si intermetallic compounds [20], which changes the solidification behavior of this alloy.

In addition, comparing between alloy 1A and alloy 4A, which have a close C content, but the former has high contents of solution-strengthening elements than the latter, it is found that the alloy with high contents of solution-strengthening elements has lower solidification temperature, lower solid solution transformation temperature, and narrower solidification range than the one with lower contents of solution-strengthening elements; see Table 3. According to the binary diagrams of Co–Cr and Co–W [21, 22], increase in the contents of the solution-strengthening elements Cr and W would decrease the transformation temperature of the solid solution. For multi-element alloy systems, the relation of the eutectic temperature to the C content is more complex than for binary alloy systems. The eutectic temperatures of alloy 1A and alloy 2A are very close, although the latter contains more C than the former, but between alloy 3A and alloy 4A the former with lower C content has higher eutectic temperature. Furthermore, alloy 3A and alloy 4A have a wider solidification range than alloy 1A and alloy 2A. This is due to the fact that alloy 1A and alloy 2A contain higher levels of Cr and W, which decreases the primary phase transformation temperature, while the eutectic temperatures of these four alloys are close, thus leading to the narrower solidification range of alloy 1A and alloy 2A.

Conclusions

Cobalt-based alloys are multi-element alloy systems. Chemical composition influences the solidification behavior of these alloys significantly. However, the effects of the constituents on the solidification behavior of these alloys

are very complex due to the multi-element constitution and the metallurgical complexity. The DSC technique provides an effective approach to investigation of this issue. The microstructural analyses of the solidified DSC samples have confirmed and explained the DSC results, helping understand these effects.

It is found that the presence and contents of carbon and boron dominate the solidification behavior of cobalt-based alloys and the effects of solution-strengthening elements are nearly negligible when the contents of the solution-strengthening elements, W, Mo, and Ni are within their saturation in the solution matrix.

Solution-strengthened alloy, which contains no carbon, has a higher solidification temperature and a narrower solidification range, compared with carbide-strengthened alloys. Addition of carbon decreases the solidification temperature and increases the solidification range. Addition of boron greatly lowers the solidification temperature. With a same level of carbon, increase in the contents of solution-strengthening elements reduces the solid solution transformation temperature and the eutectic temperature.

When molybdenum content exceeds a certain level (about 12 wt%), it forms intermetallic compounds with Co and Si when Si content is high, or with Co only when Si content is low, which changes the solidification behavior significantly. Similar to molybdenum, as nickel content reaches a certain level (about 28 wt%), it forms Ni–Si intermetallic compounds when Si content is also high.

Acknowledgement The authors are grateful for financial support from the Natural Science & Engineering Research Council of Canada (NSERC), and both financial and in-kind support from Deloro Stellite Group.

References

- Davis JR (2000) Nickel, cobalt and their alloys. ASM International, Materials Park
- Betteridge W (1982) Cobalt and its alloys. Halsted Press, Chichester
- Yu LX, Zhao YT, Yang SL, Sun WR, Guo SR, Sun XF, Hu ZQ (2010) *J Mater Sci* 45(13):3448. doi:10.1007/s10853-010-4372-0
- Curio S, Battezzati L, Johnson E, Palumbo M, Pryds N (2008) *J Mater Sci* 43(9):3253. doi:10.1007/s10853-008-2540-2
- Zuo M, Liu XF, Sun QQ (2009) *J Mater Sci* 44(8):1952. doi:10.1007/s10853-009-3287-0
- Sidhu RK, Ojo OA, Chaturvedi MC (2008) *J Mater Sci* 43(10):3612. doi:10.1007/s10853-008-2575-4
- Huang P, Liu R, Wu XJ, Yao MX (2007) *J Eng Mater Technol* 129(4):523
- Ando K, Omori T, Sato J, Sutou Y, Oikawa K, Kainuma R, Ishida K (2006) *Mater Trans* 47(9):2381
- Riddihough M (1970) *Tribology* 3(4):211
- Ashworth MA, Bryar JC, Jacobs MH, Davies S (1999) *Powder Metall* 42(3):243
- Liu R, Yao MX, Wu XJ (2004) *J Eng Mater Technol* 126:204
- Cameron CB, Ferriss DP (1975) *Anti-Corrosion Method Mater* 22(4):5
- Mason SE, Rawlings RD (1985) *J Mater Sci* 20(4):1248. doi:10.1007/BF01026320
- Raghu D, Wu JB (1977) *Mater Perform* 36(11):27
- Campos I, Ramirez G, Figueroa U, Velazquez C (2007) *Surf Eng* 23(3):216
- Campos I, Ramirez G, Figueroa U, Martinez J, Morales O (2007) *Appl Surf Sci* 253(7):3469
- Liu YN, Yang H, Tan G, Miyazaki S, Jiang BH, Liu Y (2004) *J Alloys Compd* 368(14):157
- Frenk A, Kurz W (1994) *Wear* 174:81
- Schneibel JH, Ritchie RO, Kruzic JJ, Tortorelli PF (2005) *Metall Mater Trans A* 36:525
- Maroef IS, Rowe MD, Edwards GR (2005) In: Bollinghaus Th, Herold H (eds) *Hot crack phenomena in welds*. Springer, Berlin/Heidelberg
- Baker H (1992) In: *ASM handbook*, vol 3. ASM International, Materials Park
- Davis JR (1998) *Metals handbook*. ASM International, Materials Park
- Liu R, Xu W, Yao MX, Patnaik PC, Wu XJ (2005) *Scr Mater* 53(12):1351
- Xu W, Liu R, Patnaik PC, Yao MX, Wu XJ (2007) *Mater Sci Eng A* 452–453:427